11th World Congress on Computational Mechanics (WCCM XI)
5th European Conference on Computational Mechanics (ECCM V)
6th European Conference on Computational Fluid Dynamics (ECFD VI)
E. Oñate, J. Oliver and A. Huerta (Eds)

A FINITE ELEMENT MODEL FOR THE PREDICTION OF YOUNG'S MODULUS AND COMPRESSIVE STRENGTH OF LIGHTWEIGHT CONCRETE

ETIENNE MALACHANNE*, RITA SASSINE* AND ERIC GARCIA-DIAZ*

* Centre des Materiaux des Mines d'Ales (C2MA)
Ecole des mines d'Ales
6 avenue de Clavieres, 30319 Ales, France
e-mail: etienne.malachanne@mines-ales.fr, web page: http://www.mines-ales.fr

Key words: Lightweight concrete, Mesostructure, Computational method, Elastic behavior

Abstract. In this study a numerical approach to simulate elastic behavior of lightweight concrete, is presented, at mesoscopic level. Concrete is considered as a bi- phasic material, composed of a granular skeleton dispersed in a mortar. Aggregates generation should respect a granular model. A numerical concrete sample is carried out, using three-dimensional finite element mesh. Here lightweight concretes are considered, with Youngs modulus of natural sand based mortar is higher than the modulus of the lightweight coarse aggregates. Different concretes are carried out, according to experimental studies from literature, in order to distinguish the influence of the Youngs modulus contrast, and of the concrete compacity, on mechanical behavior. After a prediction of the equivalent Young's modulus, numerical compressive tests are realized until an experimental value of compressive strength, in order to propose a rupture mode of concrete, and predict a compressive strength.

1 INTRODUCTION

Lightweight concretes have been a resurgence of interest in the past years, because of their good thermal properties [1]. Several kinds of lightweight concretes are used, but the structural concretes with lightweight coarse aggregates and natural sand are studied here. In these concretes, the density is reduced by introducing air in aggregates [2]. At mesoscopic level, concrete is described as a bi-phasic material : a group of lightweight aggregates (inclusions) is embedded in a mortar paste (matrix) [3], compounded with natural sand. The prediction of the elastic behavior of this material, depends both on elastic parameters of each phase, and on the granular skeleton. The study presented here is divided in two parts, first a determination of equivalent Young's modulus of concrete is presented. Then a predictive model of compressive strength is developed.

Some models used for the determination of the equivalent elastic behavior take into account only elastic parameters of the matrix and inclusions, and are based on the representative element behavior. The bounds of Hashin and Shtrickman [4, 5] is one of them. In the same way the three spheres model of De Larrard [6] and Le Roy [7], allows to study the influence of elastic parameters of mortar and aggregates on the equivalent behavior. Nevertheless these models are less accurate when the contrast between the moduli of inclusions and the matrix is important as shown in [8]. An other work [9] uses a microtomography image of a representative sample, to study the equivalent behavior. Homogeneization models based on the tensor of Eshelby [10] consider the shape of the particles, and the interaction between phases. For example the Mori-Tanaka model [11] uses spherical particles, as the one of Benveniste [12], when the auto-coherent model proposed by Hill [13] considers polygonal shapes. Once again,these models are less accurate when the contrast between matrix and inclusion increases, as shown in [14]. In addition, the approximation of dilute medium, used for the resolution, makes these models less accurates when the volume fraction of inclusions increases.

Another model uses a micro-mechanical model and defines equivalent elastic parmeters depending on the Young's modulus of aggregates [15].

The localisation of local stress concentration around aggregates, used for the prediction of concrete compressive strength, needs to consider the shape, the granular distribution and the location of aggregates in mortar. In this case, numerical approaches take the place of analytical ones. Numerical models, based on three-dimensional microstructures, obtained by microtomography, are among the more accurate for the reprensentation of a realistic granular skeleton [8]. The classical finite element approaches, allow to describe a material with at most a thousand of inclusions. Indeed, the high number of finite elements needed for the discretization, tends to limit the number of aggregates represented in a concrete sample, for that, as explained previously, concrete is modelised as coarse aggregates embedded in a mortar paste. Aggregates are rather represented as spheres, dispersed randomly in the mortar [16, 17]. In order to represent the mesostructure in a realistic way, a granular model could be adopted [18]. In this model, a thickness is imposed between coarse aggregates [19]. On the contrary, Ke et al [20] has developed a model using inverse analysis to predict compressive strength, taking into account interfacial transition zone, but without representation of the concrete structure. At that stage, the determination of concrete failure mode is not solved in literature. If the study cited previously [20], proposes a rupture inside aggregates by compressive strength, others explains that cracking are due to tensile stresses around aggregates [21], when the rheological serie/parallel of de Larrard [6] suggests that the concrete compressive strength is governed by the one of mortar.

The work presented in the present paper proposes a numerical model used to predict the mechanical elastic properties of concretes of lightweight aggregates. First a three-dimensional numerical model has been carried out taking into account a specific granular law. A bi-phasic lightweight concrete is generated, with a perfect mechanical link between

mortar and aggregates. After calculation and validation of the equivalent Young's modulus, the numerical model will be performed to determine stress and strain concentration around aggregates and to predict the compressive strength of concrete.

2 NUMERICAL MODEL

2.1 Generation of concrete

Concrete samples are generated as a granular skeleton of coarse aggregates, embedded in a mortar, without interfacial transition zone between them. The generation of the granular skeleton is detailed on [22]. The granular model, explained in [6], introduces the notion of maximum mortar thickness (MMT) between two coarse aggregates, depending on the volume fraction of aggregates in the sample, g, and the maximum compacity for a given mixture, g^*, defined below :

$$g^* = 1 - 0.47 \left(\frac{d_{min}}{d_{max}} \right)^{0.22} \tag{1}$$

where d_{min} and d_{max} are the minimum and maximum diameter of aggregates in the concrete sample. Thus the distance MMT can be expressed by the mathematical relationship :

$$MMT = d_{max} \left(\sqrt[3]{\frac{g^*}{g}} - 1 \right) \tag{2}$$

Using these definitions and introducing a specific granular curve [22], an algorithm allows to generate a granular skeleton at mesoscopic level. Then aggregates and mortar are meshed separately by finite elements. An example of the numerical concrete sample is presented on Figure 1.

2.2 Experimental data from literature

The numerical model presented in this study, is validated and calibrated on experimental data from works of Ke et al [15, 23, 20]. In these works, compression tests are realised on lightweight concretes, and have provided results on equivalent Young's modulus of concrete, and compressive strengths. Let us introduce these material parameters, which will be used in the following.

2.2.1 Lightweight aggregates

In the concretes considered here, Young's modulus of mortar is higher than the one of lightweight aggregates. Three lightweight aggregates are used, called 430A, 520S and 750S. Young's modulus of these aggregates are given by an empirical equation provided by the ACI Committe [24], which binds the Young's modulus of aggregates E_{agg} with their density ρ_{agg} by the relationship :

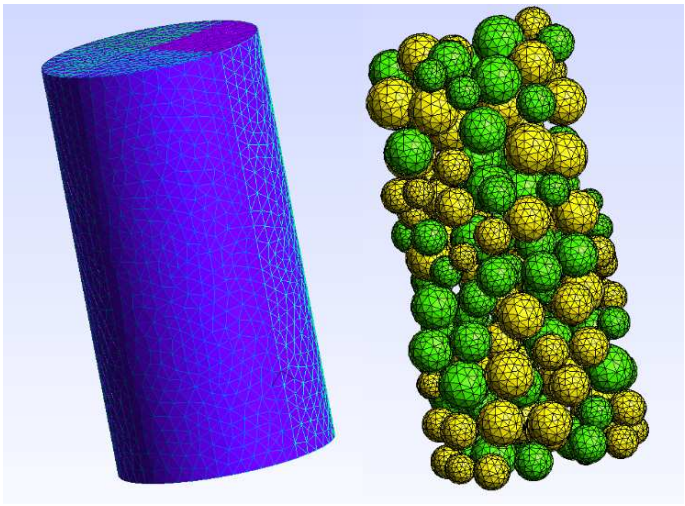

Figure 1: Concrete meshed by finite elements with a volumic fraction of 45%

$$E_{agg} = 0.008 \times \rho_{agg}^2 \tag{3}$$

Following the previous equation, Young's modulus of aggregates are summarized in the Table 1. Thus the aggregates chosen allows to consider a range of aggregates more and more rigid.

Table 1: Mechanical elastic properties of lightweight aggregates

Lightweight aggregate	ρ_{agg} (kg/m^3)	E_{agg} (GPa)
430A	737	4.3
520S	901	6.5
750S	1577	19.9

2.2.2 Mortars of natural sand

Mortars of natural sand used in the lightweight concretes modelised here, comes from experimental works of Ke et al. Indeed modulus of elasticity have been determined with compressive tests [25] until the value of mortar compressive strength. Here two mortars are selected, called M8 and M10. Values of Young's modulus E_m and compressive strengths f_{cm} of these mortars are presented on Table 2.

One can notice that mortar M10 is stronger than the M8. Moreover Ke et al [15] has observed that properties of interfacial transition zone (ITZ) are not the same for

Table 2: Mechanical properties of mortars

Mortar	E_m (GPa)	f_{cm} (MPa)
M8	28.6	40
M10	35.4	86

both mortars. If the ITZ is nonexistent for concretes with the matrix M10, microscopic observations have shown a thickness until 100 μm between aggregates and matrix M8.

2.2.3 Lightweight concretes

Lightweight concretes studied for the calibration and validation of the numerical model, come from aggregates and mortars defined previously. Thus concretes will be called M8-430A, M8-520S and M8-750S, for the ones with mortar M8, and M10-430A, M10-520S and M10-750S for mortar M10. Moreover, the volume fraction of these concretes equals to 12.5%, 37.5% and 45%. Young's modulus E_c and compressive strengths f_c coming from experimental works are recalled in Table 3.

Table 3: Mechanical properties of lightweight concretes

Concrete	**g(%)**	**E_c (GPa)**	**f_c (MPa)**
M8-430A	12.5	24.9	37.2
	37.5	17.3	27.8
	45	15.7	25.8
M8-520S	12.5	25.1	38.1
	37.5	25.3	30.5
	45	18.3	28.8
M8-750S	12.5	27.4	42.3
	37.5	25.3	43.1
	45	24.3	42.6
M10-430A	12.5	30.2	62.8
	37.5	22.3	39.4
	45	20.1	33.9
M10-520S	12.5	32.8	70.7
	37.5	24.3	47.6
	45	22	42.3
M10-750S	12.5	34.2	81.7
	37.5	32.9	75.4
	45	33	73.2

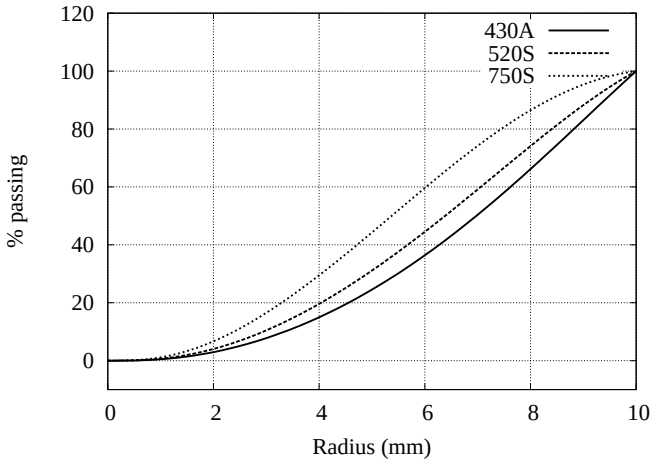

Figure 2: Granular curves of the three aggregates

3 NUMERICAL SIMULATION

The size of experimental samples are about $16 \times 32\,\text{cm}$. In order to reduce the number of finite elements generated, $4 \times 8\,\text{cm}$ numerical samples are generated and meshed with tetrahedron elements. Nevertheless the diameter of aggregates being included between 4 mm and 10 mm, the diameter of the sample is greater than three times the maximum aggregate diameter according to [26]. All the aggregates considered respect the granular curves presented by the Figure 2.

Boundary conditions are applied on each concrete sample as close as experimental study. Indeed a compression loading is applied until the experimental compressive strength of concrete.

3.1 Identification of the equivalent Young's modulus

After a compression loading applied on the 18 concretes presented in Table 3, an equivalent Young's modulus is calculated using numerical results provided by the computational simulation. Let us call σ_0 the stress applied on the lower and upper face of the sample, and ε the global strain defined as below:

$$\varepsilon = \frac{L - L_0}{L_0} \tag{4}$$

where L_0 is the initial length of the sample and L the length after the compression loading. Since the test is uniaxial and the mechanical behavior is considered elastic, the Hooke's law is reduced to the following expression :

$$E = \frac{\sigma_0}{\varepsilon} \tag{5}$$

Aggregates in the concrete sample are randomly drawing, thus in order to estimate the mean error, 4 draws have been performed, for each kind of aggregate and volume fraction.

Results are summarized in Table 4, where E_{num} is the average of the 4 Young's modulus calculated after the 4 draws, and the error calculated is the standard deviation.

Table 4: Young's modulus calculated by numerical computation

Concrete	g(%)	E_{num} (GPa)	Error (%)
M8-430A	12.5	25.7	0.9
	37.5	18.2	3.2
	45	17.9	3.1
M8-520S	12.5	26.2	0.6
	37.5	19.7	4.2
	45	17.7	2.3
M8-750S	12.5	27.8	0.7
	37.5	25.8	1
	45	25.4	0.9
M10-430A	12.5	30.9	4.1
	37.5	22.1	4.9
	45	21.5	4
M10-520S	12.5	31.3	5.8
	37.5	23.5	4.8
	45	23.5	2
M10-750S	12.5	33.8	1.8
	37.5	30.2	1.3
	45	29.7	1.3

One can notice that the maximum error due to the random draw equals to 5.8 %. The relationship between experimental Young's modulus and numerical ones, for every concretes, is represented in Figure 3. The slope of the regression curve is near 1, which allows to consider that the prediction of Young's modulus, for the lightweight concretes studied here, is quite acurate.

3.2 Prediction of rupture mode

The Young's modulus being predicted by the numerical model, let us now focus on the state of strains around aggregates. In order to visualize strains inside and around aggregates, geometrical zones are defined as shown in Figure 4. The three delimited zones, represent the center of aggregate and the core of mortar, and a geometrical zone between them. Nevertheless, as explained previously, a perfect mechanical link is considered between aggregate and mortar.

All the concrete samples are loaded until their compressive strengths, recalled in Table 3. The aggregate with the maximum diameter ($d_{max} = 10\,\text{mm}$) is isolated and the strains

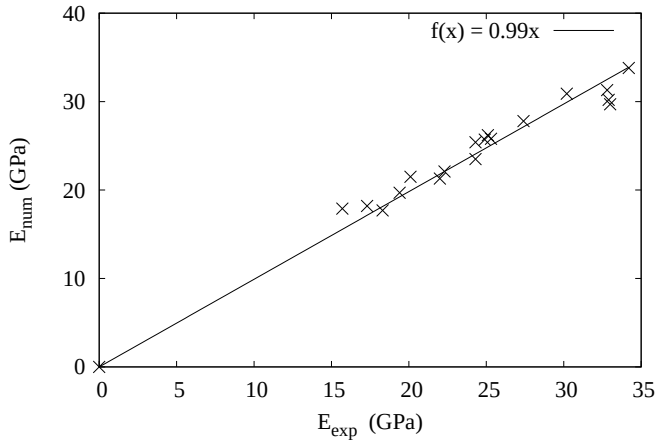

Figure 3: Comparison between experimental and numerical Young's modulus

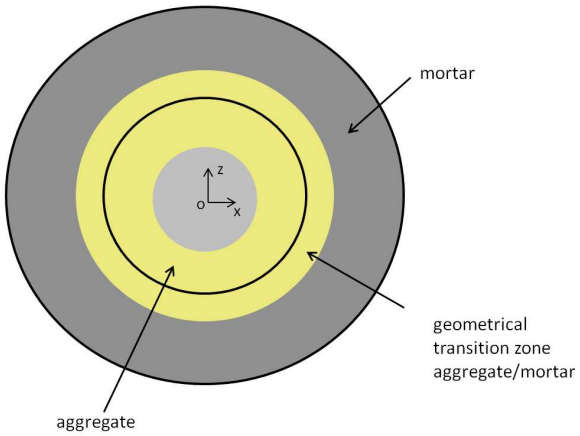

Figure 4: Geometrical zones inside and around an aggregate

are calculated in the different zones presented in Figure 4. The influence of the size and the location of the aggregate chosen in results, has been studied [27], and considered as insignificant. The evolution of the principal strain ε_1, associated with a principal axis quasi collinear with the compression axis (0,z), is presented in Figure 5. The strain is ploted along the (0,x) axis introduced in Figure 4. One can notice a convergence of strains inside mortar and inside aggregates, and peaks of strain in the geometrical transition zone, moreover when the ratio between Young's modulus of mortar aggregate is important. The curves ploted in Figure 5, present only results for concretes with mortar M10, nevertheless the same tendancy is observed for every concretes tested here. If we focus on the state of strains, it appears that means values of 1.5×10^{-3} and 2.25×10^{-3} are reached respectively in concretes with mortar M8 and M10.

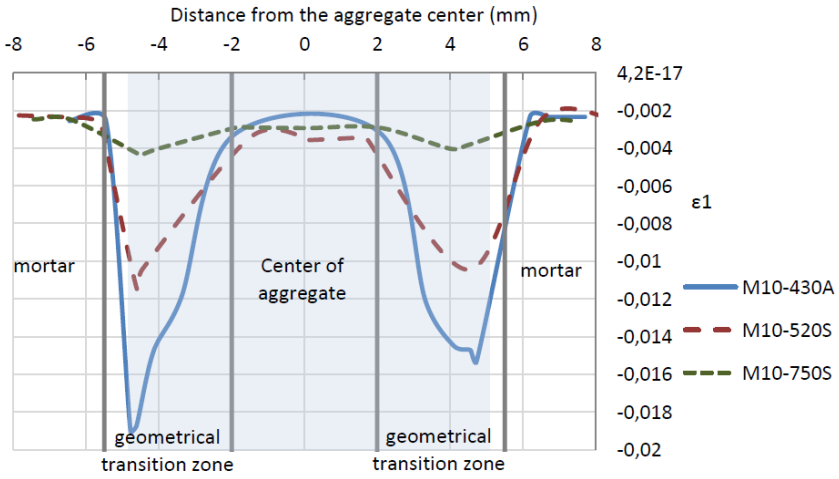

Figure 5: Strain evolution around an aggregate for concretes with mortar M10

Knowing the mechanical properties of the two mortar tested, see Table 2, it is possible to calculate the experimental maximum adimissible strain assuming that mortar is elastic until its compressive strength. These values are equal to 1.45×10^{-3} for mortar M8 and 2.45×10^{-3} for M10 and are near to these obtained by numerical simulation. Thus for a loading until the compressive strength of concrete, the maximum admissible strain is reached on mortar, for every lightweight concretes tested in this study.

3.3 Prediction of concrete compressive strength

In order to test the numerical model, boundary conditions are changed, and the numerical computation is run until the maximum admissible strain calculated previously be reached in mortar. Then the values of stress applied on upper and lower surfaces of the sample are selected and compared for each concrete to their compressive strengths. The comparison between experimental and numerical predicted compressive strengths are presented on Figure 6. A linear regression is performed with a slope equals to 1.02 and a regression coefficient about $R^2 = 0.98$.

4 DISCUSSION AND CONCLUSION

In this study, the numerical model proposed is used as a predicitve tool for mechanical behvior of lighweight concretes. Results have been focused on two mechanical parameters, the equivalent Young's modulus and the compressive strengths of the lightweight concretes tested. Intrinsic values of Young's modulus defined by the ACI [24] have been kept to perform the numerical simulation, and the prediction of the equivalent modulus of elasticity, for the 18 concretes tested, has provided a good correlation between experimental and numerical studies as shown in Figure 3. The comparison between concretes with mortar M8, which presented in experimental works an interfacial transition zone (ITZ), and the ones with mortar M10, doesn't show a noticeable difference in numerical results. Thus, for

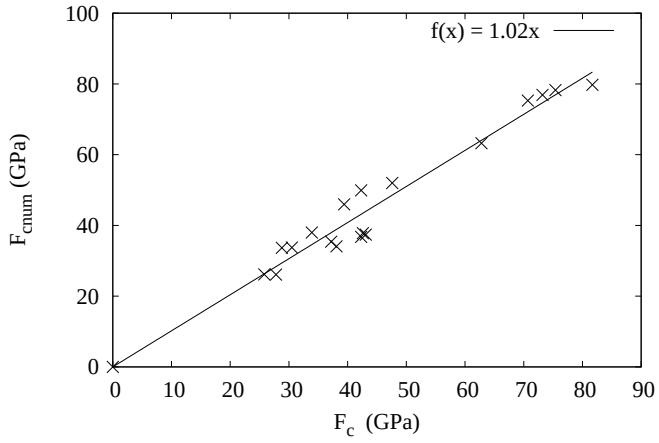

Figure 6: Comparison between experimental and numerical predicted concrete compressive strengths

the lightweight concretes considered here, the modelisation of the ITZ, which hasn't been taken into acount, doesn't influence the results. Keeping the same materials parameters for aggregates and mortars, the state of strains inside concretes, inside and aroud the aggregate with the maximum diameter, has shown that the maximum admissible strain were reached in mortar, for a lightweight concrete loaded until the compressive strength. If the other rupture modes are not eliminated, we assume that in concretes tested the unifying hypothesis is the rupture by compression inside mortar. Thus a good correlation is again found between experimental and numerical predicted compressive strength, keeping intrinsic material parameters. The mean error equals to 8.9% for concretes with mortar M10, and 9.8% for concretes with mortar M8. Once again, the lack of modelisation of an interfacial transition zone, doesn't increase the error. Nevertheless the model has to be improved, in order to take into acount damage effects.

REFERENCES

[1] J L Clarke. *Structural Lightweight Aggregate Concrete*. Blackie Academic and Professional, 1993.

[2] M. Arnould and M. Virlogeux. *Light concretes and aggregates*. Presses de l'Ecole nationale des Ponts et Chaussees, 1986.

[3] A Caballero, C M Lopez, and I Carol. 3d meso-structural analysis of concrete specimens under uniaxial tension. *Computer Methods in Applied Mechanics and Engineering*, 195(52):7182–7195, 2006.

[4] Zvi Hashin. The elastic moduli of heterogeneous materials. *Journal of Applied Mechanics*, 29(1):143–150, 1962.

[5] Z Hashin and S Shtrikman. A variational approach to the theory of the elastic behaviour of multiphase materials. *Journal of Mechanics and Physics of Solids*, 11(2):127–140, 1963.

[6] Francois De Larrard. Mixture proportioning of lightweight aggregate concrete. In *International Conference on High-Performance Concrete and Performance and Quality of Concrete Structures*, pages 154–166, 1996.

[7] R Le Roy. *Deformations instantanees et differees des betons e hautes performances*. PhD thesis, Ecole Nationale des Ponts et Chaussees (France), 1995.

[8] J Escoda, F Willot, D Jeulin, J Sanahuja, and C Toulemonde. Estimation of local stresses and elastic properties of a mortar sample by fft computation of fields on a 3d image. *Cement and Concrete Research*, 41(5):542–556, 2011.

[9] F Willot, L Gillibert, and D Jeulin. Microstructure-induced hotspots in the thermal and elastic responses of granular media. *International Journal of Solids and Structures*, 50:1699–1709, 2013.

[10] J D Eshelby. The determination of the elastic field on an ellipsoidal inclusion, and related problems. In *Royal Society*, 1957.

[11] T Mori and K Tanaka. Average stress in matrix and average elastic energy of materials with misfitting inclusions. *Acta Metallurgica and Materialia*, 21:571–574, 1973.

[12] Y Benveniste. A new approach to the application of mori-tanaka's theory in composite materials. *Mechanics of Materials*, 6(2):147–157, 1987.

[13] R Hill. A self-consistent mechanics of composite materials. *Journal of the Mechanics and Physics of Solids*, 13(4):213–222, 1965.

[14] J Sanahuja and C Toulemonde. Numerical homogenization of concrete microstructures without explicit meshes. *Cement and Concrete Research*, 41(12):1320–1329, 2011.

[15] Y Ke, A L Beaucour, S Ortola, H Dumontet, and R Cabrillac. Influence of volume fraction and characteristics of lightweight aggregates on the mechanical properties of concrete. *Construction and Building Materials*, 23(8):2821–2828, 2009.

[16] Z.M. Wang, A.K.H. Kwan, and H.C. Chan. Mesoscopic study of concrete i: generation of random aggregate structure and finite element mesh. *Computers and Structures*, 70:533 – 544, 1999.

[17] D N'Guyen, C Lawrence, C La Borderie, M Matallah, and G Nahas. A mesoscopic model for a better understanding of the transition from diffuse damage to localized damage. *European Journal of Environmental and Civil Engineering*, 14(6-7):751–776, 2010.

[18] Francois De Larrard. *Concrete Mixture Proportioning*. E&FN Spon, London and New York, 1999.

[19] I Comby-Peyrot, P-O Bouchard, F Bay, F Bernard, and E Garcia-Diaz. Numerical aspects of a problem with damage to simulate mechanical behavior of a quasi-brittle material. *International Journal of Computational Materials Science and Surface Engineering*, 40(3):327–340, 2007.

[20] Y Ke, S Ortola, A L Beaucour, and H Dumontet. Micro-stress analysis and identification of lightweight aggregates failure strength by micromechanical modeling. *Mechanics of Materials*, 68:176–192, 2014.

[21] T W Bremner. *In fluence of aggregate structure on low density concrete*. PhD thesis, Imperial college of science and technology, London, 1981.

[22] E Malachanne, R Sassine, E Garcia-Diaz, and F Dubois. Numerical model for mechanical behavior of lightweight concrete and for the prediction of local stress concentration. *Construction and Building Materials*, in press, 2014.

[23] Y Ke, S Ortola, A L Beaucour, and H Dumontet. Identification of microstructural characteristics in lightweight aggregate concretes by micromechanical modelling including the interfacial transition zone (itz). *Cement and Concrete Research*, 40(11):1590–1600, 2010.

[24] ACI Committe 213. *ACI 213R-03 Guide for Structural Lightweight-Aggregate Concrete*. American Concrete Institute, 2003.

[25] Y Ke. *Caracterisation du comportement mecanique des betons de granulats legers : experience et modelisation*. PhD thesis, University of Cergy-Pontoise (France), 2008.

[26] J M Reynouard and G Pijaudier-Cabot. *Comportement mecanique du beton*. Lavoisier, 2005.

[27] R Sassine. *Un modele numerique permettant de simuler le comportement elastique des betons legers avec prise en compte de leur mesostructure*. PhD thesis, University of Montpellier 2, 2014.